



Spin-glass behavior and magnetocaloric effect in melt-spun TbCuAl alloys

Q.Y. Dong^{a,b,*}, B.G. Shen^b, J. Chen^b, J. Shen^{b,c}, J.R. Sun^b

^a Department of Physics, Capital Normal University, Beijing 100048, People's Republic of China

^b State Key Laboratory for Magnetism, Institute of Physics, Chinese Academy of Sciences, Beijing 100190, People's Republic of China

^c Key Laboratory of Cryogenics, Technical Institute of Physics and Chemistry, Chinese Academy of Sciences, Beijing 100190, People's Republic of China

ARTICLE INFO

Article history:

Received 11 May 2010

Received in revised form

5 November 2010

Accepted 14 November 2010

by S. Das Sarma

Available online 21 November 2010

Keywords:

A. Spin-glass

C. ZrNiAl-type

D. Magnetic entropy change

E. Nonlinear susceptibility

ABSTRACT

Magnetic properties and magnetocaloric effects of amorphous and crystalline TbCuAl ribbons are investigated by measuring their ac susceptibilities including a nonlinear term and dc magnetizations. The in-phase third harmonic ac susceptibility χ'_3 is found to be negative. It can be well fitted by the expression $\chi'_3 = \tau e'_3$ at high temperatures, indicating a spin-glass behavior in amorphous TbCuAl alloy. $\Delta T_f(\omega)/[T_f(\omega)\Delta \log_{10}\omega]$, a possible distinguishing criterion to judge the presence of a spin-glass behavior is ~ 0.011 . The frequency-dependent data can be well fitted by the conventional critical slowing down law and the spin-glass transition temperature is obtained to be 20.1 K. The maximum of magnetic entropy change reaches $4.5 \text{ J kg}^{-1} \text{ K}^{-1}$ for a field change of 0–50 000 Oe, while the crystalline TbCuAl compound experiences a simple ferromagnetic-to-paramagnetic phase transition. The peak value of magnetic entropy change is obtained at the Curie temperature and reaches $14.4 \text{ J kg}^{-1} \text{ K}^{-1}$ for the same field change, which is much larger than that of amorphous TbCuAl alloy.

© 2010 Elsevier Ltd. All rights reserved.

1. Introduction

The properties of RCuAl and RNiAl ternary compounds (R = heavy rare earth, such as Gd, Tb, Dy, Ho, Er) crystallizing in the hexagonal ZrNiAl-type structure have been extensively investigated and discussed in recent years [1,2]. The TbCuAl compound shows a ferromagnetic behavior at low temperature with a Curie temperature (T_C) of 52 K [3], while the TbNiAl compound exhibits antiferromagnetic coupling with a Néel temperature of 47 K [4]. The sudden disappearance of long-range magnetic order was detected for TbNi_{1-x}Cu_xAl series with $x = 0.6$ – 0.8 [5]. One possible explanation was proposed by Ehlers et al., that is, the competition between an exchange interaction mediated by the transition-metal free 3d electrons and the RKKY interaction resulted in the frustrated state [5].

Tb is the only magnetic atom in TbCuAl alloy. Randomness of Tb in amorphous TbCuAl alloy may also lead to the disappearance of long-range magnetic order. Many disordered magnetic materials exhibit spin-glass freezing at low temperatures. The variety of experimental realizations of the spin-glass state is due to different ways in which the two main ingredients, i.e. randomness and frustration, may be present [6]. These two conditions can be easily satisfied in many amorphous alloys. So it is possible to show a

spin-glass behavior in amorphous TbCuAl alloy. Melt-spinning is a widely used method of producing amorphous material with a metastable microstructure. Crystallization in amorphous alloys is of intense interest due to their applications to nanocrystalline soft magnetic materials and nanocomposite hard magnetic materials because their physical properties vary dramatically from their bulk counterparts. In this paper we report on the spin-glass properties of amorphous TbCuAl ribbons by means of measuring their ac magnetic susceptibilities including a nonlinear term and dc magnetizations, as well as the magnetic entropy change (ΔS) in amorphous and crystalline TbCuAl ribbons.

2. Experiments

The TbCuAl ingot was prepared by arc melting Tb and Cu, each with a purity of 99.9%, and Al, with a purity of 99.99%, in high purity argon atmosphere. Repeated turning over and melting were performed to ensure homogeneity. Ribbon-shaped samples were obtained by the ordinary melt-spun technique at a speed of 50 m/s. Differential scanning calorimetry (DSC) for the as-spun ribbons was carried out with a heating rate of 10 K/min. There was an exothermic peak appearing at 662 K in the DSC curve (see Fig. 1), indicating crystallization at that temperature and confirming the presence of a large number of amorphous phases in the as-spun ribbons. Post-annealing of the products at 793 K for 87 h and subsequent quenching to room temperature were performed to obtain crystalline samples. The structures of samples were characterized by an X-ray diffractometer with

* Corresponding author at: Department of Physics, Capital Normal University, Beijing 100048, People's Republic of China. Tel.: +86 10 68907979.

E-mail address: happy1augh746@gmail.com (Q.Y. Dong).

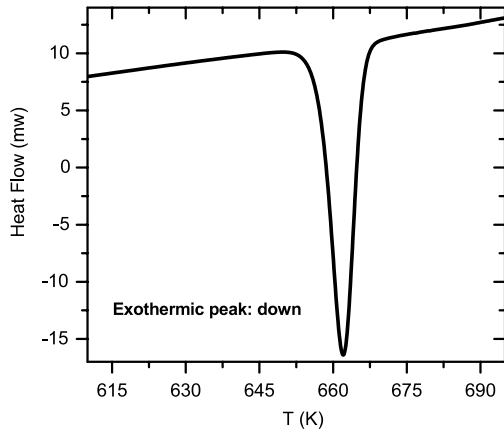


Fig. 1. DSC curve of TbCuAl ribbons melt-spun at a speed of 50 m/s.

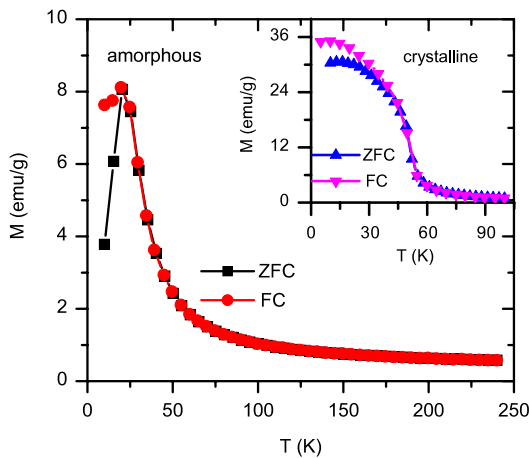


Fig. 2. Temperature dependence of the ZFC and FCC magnetizations for amorphous TbCuAl alloy under a field of 1000 Oe. The inset shows the dependence of ZFC and FCC magnetizations on temperature for crystalline TbCuAl compound.

Cu K_{α} radiation. X-ray diffraction results indicate that the as-spun ribbons are amorphous while the annealed ribbons are crystallized in a nearly single phase with a hexagonal ZrNiAl-type structure (space group $P6_3/mmc$). The lattice parameters are found to be $a = 7.029 \text{ \AA}$ and $c = 4.034 \text{ \AA}$ which are almost in agreement with the experimental results reported by Javorsky et al. [1]. All magnetic measurements were performed on a commercial Physical Property Measurement System (PPMS, Quantum Design) and a commercial MPMS-7 superconducting quantum interference device magnetometer (Quantum Design). The ac magnetic susceptibility was recorded in the warming process for frequencies between 10 and 497 Hz and under an alternating field of 10 Oe. The value of ΔS was calculated by the Maxwell relation based on magnetization data [7].

3. Results and discussion

Fig. 2 and its inset show the zero-field cooling (ZFC) and field-cooling (FC) temperature dependence of magnetization M under a field of 1000 Oe for amorphous and crystalline TbCuAl samples, respectively. Crystalline ribbons exhibit a typical ferromagnetic-paramagnetic transition at $\sim 52 \text{ K}$ as reported previously [3]. The irreversibility between the ZFC and FC branches at low temperature can be observed. It has been revealed that the TbCuAl compound possesses a canted ferromagnetic structure, i.e. all the spins of Tb^{3+} ions align in parallel and make a small angle (20°) with respect to the c -axis [4]. This “close to uniaxial” anisotropy

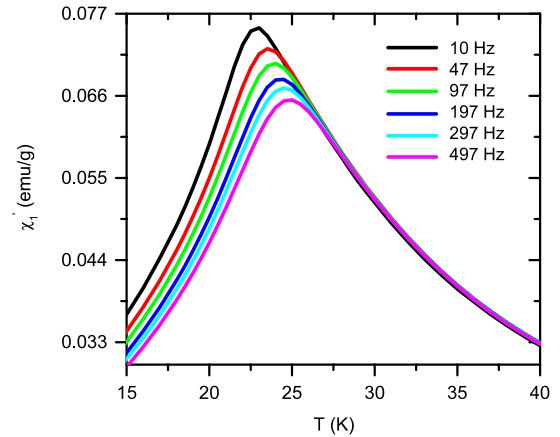


Fig. 3. Temperature dependence of χ_1' for amorphous TbCuAl alloy under a zero dc field at different frequencies.

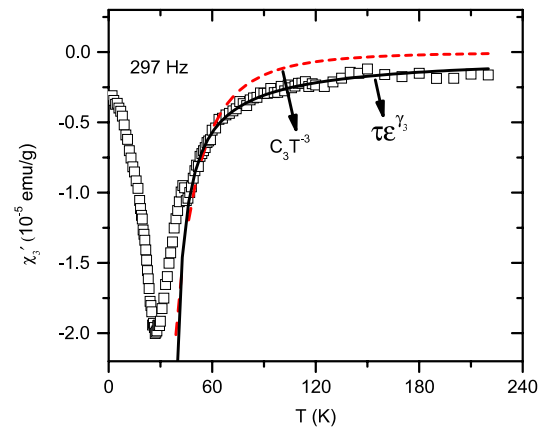


Fig. 4. Temperature dependence of χ_3' for amorphous TbCuAl alloy at 297 Hz, measured under a zero dc field. The dotted line denotes the fitting to $C_3 T^{-3}$, and the solid line represents the fitting to $\tau \epsilon_3^{\gamma_3}$.

leads to the divergence between ZFC and FC branches at low temperatures. In contrast, for amorphous ribbons a small cusp centered at about 20 K is observed in the ZFC curve, while a well-pronounced ZFC–FC splitting can be seen at lower temperatures.

Fig. 3 shows the temperature dependence of the real part of first harmonic ac magnetic susceptibility χ_1' for amorphous TbCuAl alloy at six frequencies ranging from 10 to 497 Hz. One can find that each curve shows a peak which obviously shifts toward higher temperatures with the increase of frequency. Both the superparamagnetic and spin-glass-like systems own this feature. To further confirm which behavior the amorphous TbCuAl alloy shows, the measurement of the nonlinear ac magnetic susceptibility was performed. The third harmonic (χ_3) is used to distinguish the superparamagnetic or the spin-glass-like behaviors, which are similar for the first harmonic [8]. Although χ_3' (the real part of χ_3) is negative in both cases, it varies with $1/T^3$ above the blocking temperature (T_B) when superparamagnetism is predominant [8,9]. In contrast, for a spin-glass system, χ_3' is given by $-\chi_3' = \tau \epsilon_3^{\gamma_3}$ above the glass transition temperature (T_{SG}) [8,10], where ϵ is $(T - T_{SG})/T_{SG}$, γ_3 the critical exponent, and τ the relevant critical amplitude. Fig. 4 displays the real part of χ_3 as a function of temperature for amorphous TbCuAl ribbons at 297 Hz, measured under an ac field of 10 Oe. χ_3' is negative and shows a minimum at $\sim 27 \text{ K}$. Furthermore, $\tau \epsilon_3^{\gamma_3}$ can well describe the $\chi_3' \sim T$ curve above 40 K, while the fitting line distinctly deviates from the experimental data by using $C_3 T^{-3}$, where C_3 is the fitting parameter. These results confirm the spin-glass-like

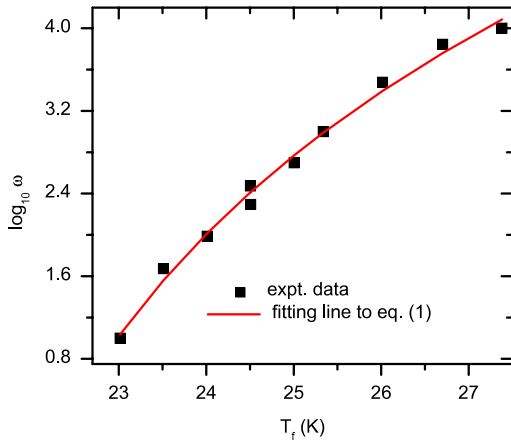


Fig. 5. Frequency dependence of the freezing temperature T_f for amorphous TbCuAl alloy. The solid line denotes the best fitting to expression (1).

character of amorphous TbCuAl alloy. Thus the peak temperature in Fig. 3 corresponds to the spin-glass freezing temperature $T_f(\omega)$. The frequency sensibility of $T_f(\omega)$, represented by $\Delta T_f(\omega)/[T_f(\omega)\Delta \log_{10}\omega]$, is determined to be ~ 0.011 , which is close to that of a conventional spin glass system [11]. In amorphous TbCuAl alloy, Tb is the only magnetic atom. It is of the positional randomness that creates a Tb-spin distance distribution which is the first and basic ingredient of a spin-glass behavior. The oscillating RKKY interaction is operative in its usual competing-exchange form. The combination of site disorder with the positive and negative RKKY interactions causes a mixture of competitive bonds that will eventually lead to frustration in some of these bonds, which produces the spin-glass behavior [12].

Taking the temperature corresponding to the cusp of the in-phase ac magnetic susceptibility as the onset of the strong irreversibility of each measurement time $t_{\text{meas}} = 1/\omega$ (ω being the frequency of the ac magnetic field) and studying the dependence of T_f on ac field frequency, the dynamic properties of a true phase transition can be checked [13]. The divergence of the maximum relaxation time, occurring at the spin-glass transition temperature T_{SG} , can be investigated by using the conventional critical slowing down [14]:

$$\omega = \omega_0 \left(\frac{T_f(\omega) - T_{\text{SG}}}{T_{\text{SG}}} \right)^{zv}, \quad (1)$$

where zv is the dynamic exponent. A best fit of the measured data to expression (1) is shown in Fig. 5, yielding the values $zv = 7.63$, and $T_{\text{SG}} = 20.1$ K which well corresponds to the dc (equilibrium) value of $T_{\text{SG}}(\omega \rightarrow 0)$ (see Fig. 2). The value of zv is a typical value for conventional spin glass [13].

Fig. 6 displays the temperature dependence of the in-phase component of the linear magnetic susceptibility (χ'_1) for amorphous TbCuAl alloy in various dc magnetic fields (from 50 to 5000 Oe) and at 50 Hz of ac frequency. A sharp cusp is observed at about 24 K when the applied field is low. However, it smears out and shifts toward low temperatures with the increase of external field, which is similar to other reported results for spin-glass systems [15,16].

As an example, the inset of Fig. 7 shows the ZFC isothermal magnetization curve at 2 K. The full saturation state cannot be achieved even under a field of 5 T. It can be interpreted as follows. In spin-glass systems, each spin is frozen along its own anisotropic axis below the freezing temperature. Moreover, the distribution of anisotropic axes is random. In order to make the direction of spins accordant with the increase of the applied field, the energy barrier between the external field and the

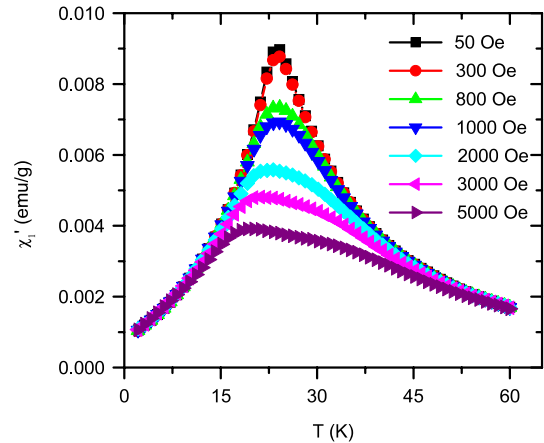


Fig. 6. Temperature dependence of χ'_1 for amorphous TbCuAl alloy under an ac frequency of 50 Hz in different magnetic fields.

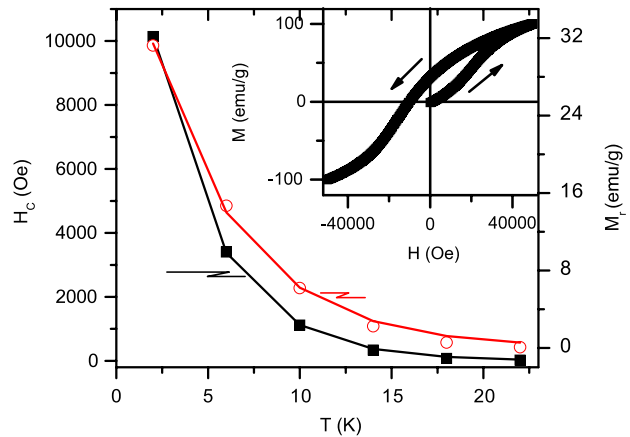


Fig. 7. Temperature dependence of coercive field H_c and remanent magnetization M_r for amorphous TbCuAl alloy. The inset shows the magnetization curve at 2 K.

anisotropic axis must be overcome. However, the heights of energy barriers are different. Thus, it is difficult for spin-glass systems to achieve the full saturation state. Fig. 7 exhibits the temperature dependence of coercive field H_c and remanent magnetization M_r based on the ZFC hysteresis loops at different temperatures for amorphous TbCuAl alloy. Both H_c and M_r increase with lowering temperature below T_f , which is in accordance with those observed in other spin-glass systems [17,18]. They can be well fitted to the exponential functions $H_c(T) = H_{c0} \exp(-\alpha T)$ and $M_r(T) = M_{r0} \exp(-\beta T)$, respectively. The best agreement is achieved for $H_{c0} = 17592.7$ Oe, $\alpha = 0.275$ K $^{-1}$, $M_{r0} = 47.15$ emu/g, and $\beta = 0.203$ K $^{-1}$.

The magnetocaloric property of amorphous TbCuAl alloy was investigated by measuring the initial isothermal magnetizations at different temperatures. It is worth mentioning that the data were recorded after cooling under a zero field from 100 K (above T_f) to the measured temperature. For comparison, the magnetocaloric effect of crystalline TbCuAl compound was also studied. Fig. 8(a) and (c) show the Arrott plots of amorphous TbCuAl alloy and crystalline TbCuAl compound, respectively. S-shaped curves are observed in amorphous TbCuAl alloy below T_f , and the inflection point shifts toward high values of H/M with decreasing temperature, which is one of the properties of spin-glass systems [19]. No positive intercepts at any temperature in Arrott plots further confirm the nonexistence of long-range order in amorphous TbCuAl alloy. The Arrott plots of crystalline TbCuAl compound indicate that a second-order ferromagnetic–paramagnetic phase transition takes place at $T_c = 52$ K because the indication of the evidence for

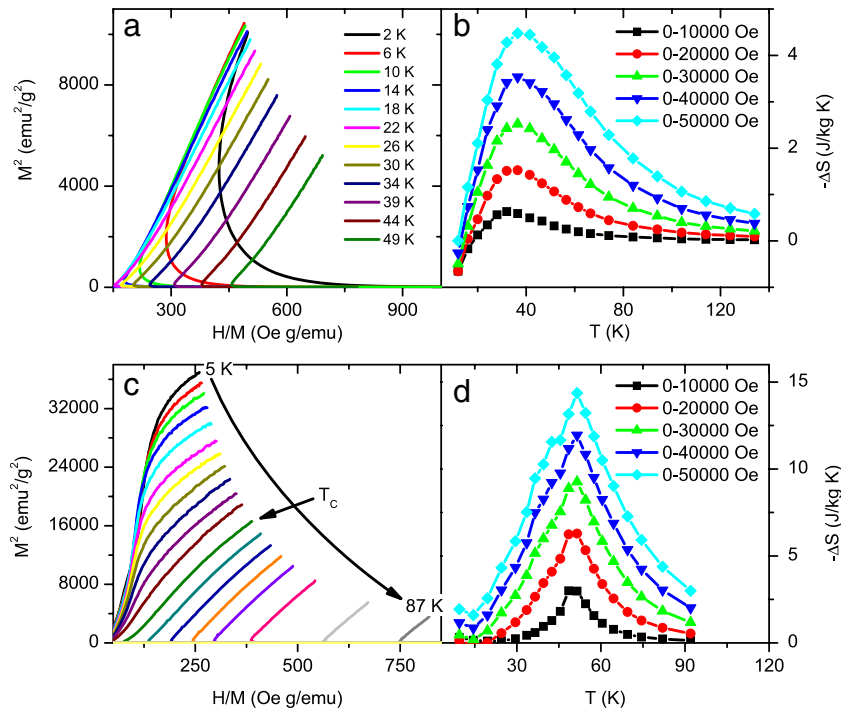


Fig. 8. Arrott-plots and temperature dependence of magnetic entropy change under typical field changes for amorphous TbCuAl alloy ((a) and (b)) and for crystalline TbCuAl alloy ((c) and (d)), respectively.

a typical first-order phase transition to emerge, such as a negative slope or an obvious inflection point [20,21], is not observed. Fig. 8(b) and (d) show the temperature dependences of the magnetic entropy changes under typical field changes for amorphous TbCuAl alloy and crystalline TbCuAl compound, respectively. Under a field change of 0–50 000 Oe, the maximum of $-\Delta S$ reaches $4.5 \text{ J kg}^{-1} \text{ K}^{-1}$ at 36 K for amorphous TbCuAl alloy, which is associated with the spin-glass transition. This value is smaller than those of Tb-based bulk metallic glasses ever reported ($7.5 \text{ J kg}^{-1} \text{ K}^{-1}$ for $\text{Tb}_{55}\text{Co}_{20}\text{Al}_{25}$ [22], $8.0 \text{ J kg}^{-1} \text{ K}^{-1}$ for $\text{Gd}_{0.32}\text{Tb}_{0.26}\text{Co}_{0.20}\text{Al}_{0.22}$ [23]), which may be caused by the lower rare earth concentration in amorphous TbCuAl alloy. For crystalline TbCuAl compound, the peak value of $-\Delta S$ appears at T_c , and it approaches $14.4 \text{ J kg}^{-1} \text{ K}^{-1}$ under the same field change, which is much larger than that for amorphous TbCuAl alloy. It is also larger than that of the TbCoAl compound ($12.5 \text{ J kg}^{-1} \text{ K}^{-1}$) [24].

4. Conclusions

Magnetic properties and magnetocaloric effects of amorphous TbCuAl alloy and crystalline TbCuAl compound are investigated. The ac magnetic susceptibility including nonlinear components and the dc magnetization data bear signatures of a spin-glass state in amorphous TbCuAl alloy. The frequency ω -dependent freezing temperature T_f varies as $\Delta T_f(\omega)/[T_f(\omega)\Delta \log_{10} \omega] \approx 0.011$, which is in good agreement with the reported values for other spin-glass systems. T_{SG} is obtained to be 20.1 K by fitting the frequency-dependent data according to the critical slowing down law. The thermal and magnetic hystereses are observed below T_f . Both the coercive field and the remanent magnetization, obtained from the isothermal magnetic hysteresis loops, decrease exponentially with increasing temperature. Under a field change of 0–50 000 Oe, the maximum of magnetic entropy change reaches $4.5 \text{ J kg}^{-1} \text{ K}^{-1}$, while for the crystalline TbCuAl compound, it displays a ferromagnetic–paramagnetic phase transition. The maximum of magnetic entropy change is obtained at T_c and reaches $14.4 \text{ J kg}^{-1} \text{ K}^{-1}$ for the same field change.

Acknowledgements

This work is supported by the National Natural Science Foundation of China (Grant No. 50731007 and 51001077), the National Basic Research Program of China (Grant No. 2006CB601101), the Knowledge Innovation Project of the Chinese Academy of Sciences, and the opening project of the Key Laboratory of Cryogenics Technical Institute of Physics and Chemistry, Chinese Academy of Sciences.

References

- [1] P. Javorsky, L. Havela, V. Sechovsky, H. Michor, K. Jurek, J. Alloys Compd. 264 (1998) 38.
- [2] J. Prchal, P. Javorsky, J. Ruzs, F. de Boer, M. Divis, H. Kitazawa, A. Donni, S. Danis, V. Sechovsky, Phys. Rev. B 77 (2008) 134106.
- [3] K. Binder, K. Schroder, Phys. Rev. B 14 (1976) 2142.
- [4] G. Ehlers, H. Maletta, Z. Phys. B 99 (1996) 145.
- [5] G. Ehlers, D. Ahlert, C. Ritter, W. Miekeley, H. Maletta, Europhys. Lett. 37 (1997) 269.
- [6] J.L. Tholence, A. Mauger, M. Escorne, R. Triboulet, Solid State Commun. 49 (1984) 417.
- [7] K.A. Gschneidner Jr., V.K. Pecharsky, Phys. Rev. Lett. 78 (1997) 4494.
- [8] A. Banerjee, A. Bajpai, S. Nair, in: Narlikar, A.V. (Eds.), Frontiers in Magnetic Materials, Berlin, 2005, pp. 43–69.
- [9] A. Bajpai, A. Banerjee, Phys. Rev. B 62 (2000) 8996.
- [10] S. Fujiki, S. Katsura, Progr. Theoret. Phys. 58 (1981) 1130.
- [11] J.A. Mydosh, Spin Glasses: An Experimental Introduction, Taylor and Francis, London, 1993, p. 67.
- [12] J.A. Mydosh, Spin Glasses: An Experimental Introduction, Taylor and Francis, London, 1993, pp. 3–9.
- [13] B. Martinez, A. Labarta, R. Rodriguez-Sola, X. Obradors, Phys. Rev. B 50 (1994) 15779.
- [14] A.T. Ogielski, I. Margenstern, Phys. Rev. Lett. 54 (1985) 928.
- [15] G.F. Zhou, H. Bakker, Phys. Rev. Lett. 73 (1994) 344.
- [16] J. Mantilla, E. Ter Haar, J.A.H. Coaquira, V. Bindilatti, J. Phys.: Condens. Matter 19 (2007) 386225.
- [17] K. Binder, A.P. Young, Rev. Modern Phys. 58 (1986) 801.
- [18] J. Dho, W.S. Kim, N.H. Hur, Phys. Rev. Lett. 89 (2002) 027202.
- [19] H. Maletta, W. Felsch, Phys. Rev. B 20 (1979) 1245.
- [20] H. Yamada, Phys. Rev. B 47 (1993) 11211.
- [21] H. Saito, T. Yokoyama, K. Fukamichi, J. Phys.: Condens. Matter 9 (1997) 9333.
- [22] J. Du, Q. Zheng, E. Bruck, K.H.J. Buschow, W.B. Cui, W.J. Feng, Z.D. Zhang, J. Magn. Mater. 321 (2009) 413.
- [23] Y.S. Liu, J.C. Zhang, Y.Q. Wang, Y.Y. Zhu, Z.L. Yang, J. Chen, S.X. Cao, Appl. Phys. Lett. 94 (2009) 112507.
- [24] X.X. Zhang, F.W. Wang, G.H. Wen, J. Phys.: Condens. Matter 13 (2001) L747.